

Phase Behavior of Polystyrene and Poly(*n*-pentyl methacrylate) Blend

Du Yeol Ryu, Min Soo Park, Seung Hun Chae, Jin Jang, and Jin Kon Kim*

Department of Chemical Engineering, Polymer Research Institute, Electronic and Computer Engineering Divisions, Pohang University of Science and Technology, Kyungbuk 790-784, Korea

Thomas P. Russell

Department of Polymer Science and Engineering, University of Massachusetts, Amherst, Massachusetts 01003

Received August 1, 2002

Revised Manuscript Received September 11, 2002

The phase behavior of polymer blends has been studied extensively,^{1–19} both experimentally and theoretically. Two types of phase transitions have been reported on the basis of the temperature dependence of the segmental interaction parameter, χ : the upper critical solution temperature (UCST), the temperature above which two polymers mix, and the lower critical solution temperature (LCST), the temperature above which two polymers phase separate.^{1,2} Although the coexistence of both transitions (UCST at lower temperatures and LCST at higher temperatures) is predicted theoretically,³ both transitions have not been observed for a single bulk homopolymer mixture, although mixtures of a homopolymer and solvent⁴ and mixtures of a copolymer and a homopolymer^{5,6} that exhibit both transitions have been studied. Hammouda et al.⁷ showed that blends of deuterated polystyrene (dPS) and poly(*n*-butyl methacrylate) (PnBMA) appeared to have both UCST and LCST, since the zero-angle small-angle neutron scattering (SANS) intensity of homogeneous mixtures exhibited a minimum as a function of temperature. However, clear evidence of both UCST and LCST for this mixture was not observed. On the other hand, PS-*block*-PnBMA block copolymers have been shown to exhibit both the order-to-disorder transition (ODT) at lower temperatures and disorder-to-order transition (LDOT) at higher temperatures, although the former was barely discernible experimentally due to the encroachment of the T_g of PS block.⁸

Mayes et al.^{15,16} developed a compressible, regular solution theory that showed good agreement with experimental data for PS-poly(*n*-alkyl methacrylate) diblock copolymers. Depending upon the relative magnitude of the mean-field (incompressible) free energy to the entropic contribution of the free energy resulting from the differences in the thermal expansion coefficients of blend components, this theory predicts that some blend systems exhibit only UCST behavior, whereas other blends should exhibit both UCST and LCST behaviors.

Very recently, the diblock copolymer of PS and poly(*n*-pentyl methacrylate) (PS-PnPMA) was shown to exhibit a closed loop type phase behavior, where, upon heating, a disorder-to-order transition (LDOT) was found at lower temperatures, and an upper order-to-disorder transition (UODT) was observed at higher temperatures.²⁰ According to mean-field arguments, the phase behavior of a polymer blend should be related to

that of the corresponding block copolymer provided one takes into account the differences in the molecular weights to satisfy the critical conditions. In this communication, the phase behavior of the PS/PnPMA blend is discussed, as determined by turbidity measurements and small-angle neutron scattering (SANS). These are compared to the phase behavior of PS-PnPMA diblock copolymer.

Two polystyrenes (PS-L and PS-H) and d-PS were synthesized anionically in tetrahydrofuran (THF) at -78°C under purified argon using *sec*-BuLi as an initiator. Three PnPMAs (PnPMA-L, PnPMA-M, PnPMA-H) were synthesized anionically in THF containing excess dried LiCl at -78°C using another initiator prepared by *sec*-BuLi and 1,1-diphenylethylene. The number- and weight-average molecular weights, M_n and M_w , respectively, of all the homopolymers used in this study were measured by multiangle laser light scattering (MALLS) combined with size exclusion chromatography (SEC) and are given in Table 1. Since the phase behavior is so sensitive to the molecular weight (M), two other PSs (PS-BH and PS-BL) were made by blending of high (PS-H) and low (PS-L) molecular weights. Since the M_w 's for PS-H and PS-L differ by only 7.5% and their polydispersity (M_w/M_n) are less than 1.03, M_w/M_n 's for PS-BH and PS-BL were also ~ 1.03 . Consequently, the PS-BL and PS-BH can be treated as homopolymers.

Various blend compositions for the turbidity temperature (T_b) measurements were prepared by dissolving a predetermined amount of the mixtures in toluene (10 wt % in solute) and slowly evaporating the solvent over 8 h at room temperature. The sample thickness was $\sim 10\ \mu\text{m}$. Each specimen was annealed in the homogeneous state ($\sim 130^\circ\text{C}$) for 4 h. The T_b of each blend was determined by optical microscopy (OM, Axioplan, Zeiss Co.) using a heating block blanketed in nitrogen. The T_b 's for the LCST were first estimated by the threshold temperature, above which phase-separated structures were clearly seen under the OM with a magnification of $400\times$ upon heating at a rate of $0.5^\circ\text{C}/\text{min}$. The T_b 's for the UCST were similarly estimated on cooling at a rate of $0.5^\circ\text{C}/\text{min}$. Once T_b of a specimen was estimated, the exact T_b was determined by OM with a stepwise change of 0.5°C near the T_b . The specimen was held at a temperature for 1 h for the measurement of the LCST and for 10 h for the measurement of the UCST due to the proximity of the glass transition temperatures (T_g) of the blend. The maximum error in the values of T_b determined would be less than $\pm 0.5^\circ\text{C}$.

The T_g 's of the blend samples were measured using a Perkin-Elmer DSC 7 differential scanning calorimeter. Prior to measurement, the baseline was established using two empty pans. To prevent thermal degradation, nitrogen gas was circulated around the sample pan. The DSC thermograms were obtained during the first heating run at $10^\circ\text{C}/\text{min}$ for blends and during the second heating run for homopolymers.

Samples for SANS were prepared by compression-molding plaques at 100°C , followed by annealing at 100°C for 24 h under vacuum. SANS experiments were performed at the Hanaro Reactor (Korea) with a wavelength (λ) of 0.431 nm and $\Delta\lambda/\lambda = 0.12$ at a sample-to-detector distance of 3 m. Scattering intensities were collected on a 2-D area detector and then circularly

* To whom correspondence should be addressed. E-mail: jkkim@postech.ac.kr.

Table 1. Molecular Characteristics of PS, d-PS, and PnPMA Homopolymers and dPS–PnPMA Block Copolymers Employed in This Study

sample code	M_n	M_w	M_w/M_n^a
PS-L	6610	6810	1.03
PS-BL ^b	6835		
PS-BH ^b	6960		
PS-H	7110	7270	1.02
d-PS	9150	9250	1.02
PnPMA-L	7570	7700	1.02
PnPMA-M	7900	8030	1.02
PnPMA-H	8480	8650	1.02
dPS–PnPMA-L ^c	46000	47500	1.03
dPS–PnPMA-BH ^c	50000	51000	1.02

^a Measured by multiangle laser light scattering combined with SEC. ^b PS-BL and PS-BH were prepared by blending of PS-H and PS-L. The weight fractions of PS-H and PS-L are 0.45/0.55 in PS-BL and 0.70/0.30 in PS-BH, respectively. ^c The volume fraction of dPS block is 0.5.

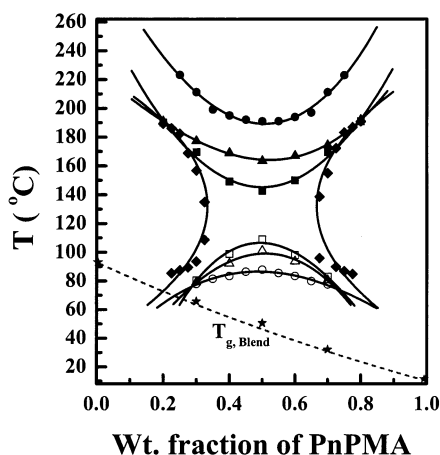


Figure 1. Phase diagrams of PS/PnPMA-L blends with different molecular weights of PS: PS-L (●, ○), PS-BL (▲, △), PS-BH (■, □), PS-H (◆, ◇). Closed and open symbols represent the LCST and UCST curves, respectively. Plots of $T_{g,blend}$ (★) vs blend composition are added, which are obtained during the first heating run after being annealed in the homogeneous state. The dashed curve of $T_{g,blend}$ is the prediction by the Fox equation.

averaged. The sample thickness was 1.0 mm, and the exposure time was 30 min.

Cloud point curves for PS/PnPMA-L with four different molecular weights of PS are shown in Figure 1. Since the molecular weights and densities of PS and PnPMA are similar, the critical volume fraction of PnPMA was found to be ~ 0.5 . For lower molecular weights of PS (PS-L, PS-BL, PS-BH), both UCST and LCST are seen. Thus, the specimens become homogeneous at temperatures between the UCST and the LCST. It should be noted that the UCST was measurable at temperatures below the T_g of PS-H ($\sim 90^\circ\text{C}$), since the blend T_g in homogeneous state was lower than the T_b , as indicated by the dashed curve in Figure 1. The degradation temperature for PnPMA was found to be $\sim 270^\circ\text{C}$. The phase diagram given in Figure 1 was also complemented by the DSC results shown in Figure 2. When the 50/50 wt/wt PS-L/PnPMA-L blend was annealed at 210 or 78°C , temperatures where the mixture was phase-separated, for 24 h, the T_g 's corresponding to PS-rich and PnPMA-rich phases are observed. However, for the 50/50 wt/wt PS-L/PnPMA-L blend annealed at 140°C , a temperature where the blend mixes, for 24 h, only one glass transition is seen.

From Figure 1, it is seen that only a 7.5% increase in M_n of PS changes the phase behavior of a mixture with both a UCST and LCST to one with an hourglass-type phase behavior. This is understandable since, with in-

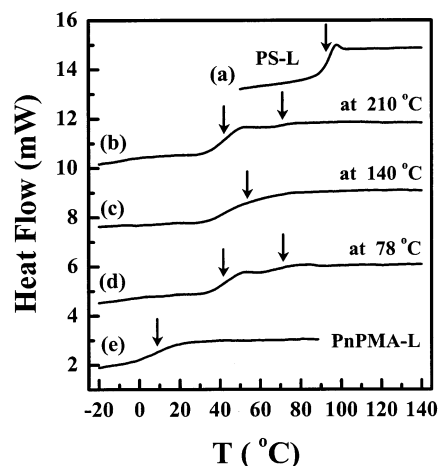


Figure 2. DSC thermograms of 50/50 (wt/wt) PS-L/PnPMA-L blends annealed at three different temperatures (curves b–d) as well as for neat PS-L (a) and neat PnPMA-L (e). Arrows indicate the midpoint of heat flow during the transition.

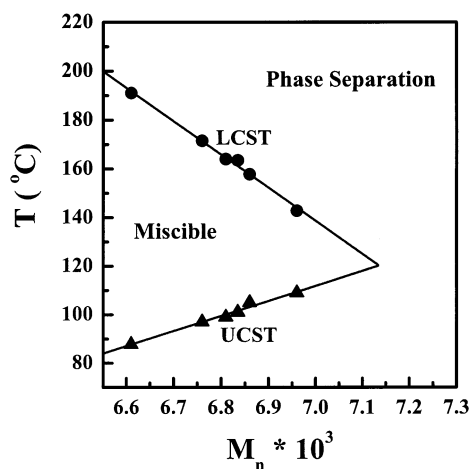


Figure 3. Changes of LCST and UCST with molecular weight of PS for 50/50 (wt/wt) PS/PnPMA-L blends.

creasing PS molecular weight, the UCST increases and the LCST decreases, and these two merge into an hourglass-type phase diagram. It was also noted that the decrease in the LCST with increasing PS molecular weight was larger than that of the UCST, as shown in Figure 3. The phase behavior of PS/PnPMA given in Figure 1 is very similar to that of PS/cyclohexane solution.⁴ However, this type of phase behavior has not been reported in mixtures of two homopolymer blends. Mixtures of a copolymer and a homopolymer^{5,6} were found to exhibit both UCST and LCST, but an hourglass phase diagram has not been reported.

The phase behavior of PS–PnPMA diblock copolymer is completely different from the phase behavior of PS/PnPMA blends reported here. A closed loop phase diagram was reported recently for the block copolymer.²⁰ It is noted from Figure 1 that the closed loop type of phase diagram might be expected when the molecular weights of PS (or PnPMA) become smaller. However, as shown in Figure 1, it is not possible to observe the UCST at higher temperatures because of sample degradation at $\sim 270^\circ\text{C}$. To reconcile the seemingly contradictory behavior between the blend and block copolymer, we employed SANS experiments after PS was labeled with deuterium. d-PS/PnPMA-M blends were prepared that have both a UCST at 71°C and a LCST at 133°C .²¹ As expected, d-PS/PnPMA-H whose M_n is just 7% greater than that of PnPMA-M showed an hourglass-

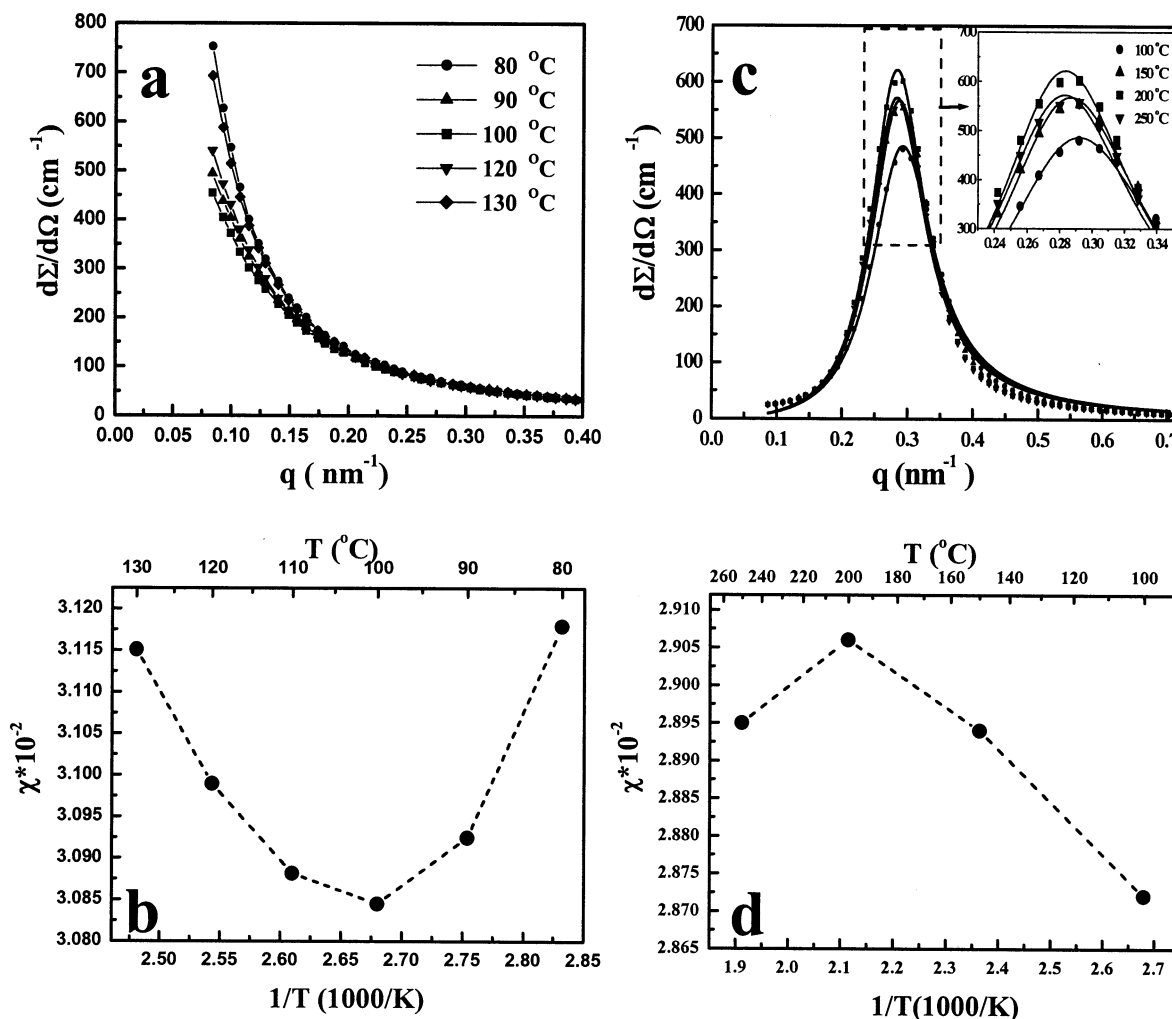


Figure 4. (a, b) SANS profiles [$I(q)$ vs q] and χ at various temperatures for 50/50 (wt/wt) dPS/PnPMA-M blend. (c, d) SANS profiles and χ at four different temperatures for dPS-PnPMA-L block copolymer.

type phase diagram. Because of the effect of the deuterium substitution on χ ,¹⁷ the UCST and LCST of dPS/PnPMA-M blend are different from those for PS/PnPMA blend. SANS was performed for 50/50 (wt/wt) dPS/PnPMA-M blend as a function of increasing temperature from 80 to 130 °C. Figure 4a shows the SANS profiles at several temperatures. It is seen that with increasing temperature the SANS intensity ($I(q)$) at all wavelengths (0.08–0.7 nm⁻¹) first decreased, went through a minimum, and then increased again. The temperature (~97 °C) corresponding to a minimum SANS intensity was slightly lower than the midpoint (102 °C) between the UCST and LCST of d-PS/PnPMA. From Figure 4a, $I(q=0)$ was determined using the Ornstein–Zernike equation.²² Using the incompressible random phase approximation (RPA) theory due to de Gennes,²² the values of χ shown in Figure 4b were obtained. It is seen that, with increasing T (or decreasing $1/T$), χ first decreases, goes through a minimum, and then increases again. Since a standard expression of χ ($\chi = a + b/T$) cannot describe these observations, the data were empirically fit with $\chi = a + b/T + c/T^2$,¹⁸ yielding $a = 0.104$, $b = -55.0$, and $c = 10355.6$. Since $c > 0$, this blend with higher M_w exhibits an hourglass type of phase behavior.

The SANS profiles for dPS-PnPMA-L at four different temperatures are shown in Figure 4c. Using the incompressible RPA theory for block copolymer,²³ the values of χ shown in Figure 4d were obtained. As can

be seen, the fits of the incompressible RPA theory are not exact, but they do provide insight into the temperature dependence of χ . While incorporating the contribution of fluctuations²⁴ to χ may improve the fits, the trends in χ with T would not change. The dPS-PnPMA-L block copolymer was disordered at temperatures studied.²¹ By slightly increasing the M_w (~10%), dPS-PnPMA-BH exhibited both LDOT at 170 °C and UODT at 250 °C.²¹ As shown in Figure 4c,d, $I(q_{\max})$ and χ increased initially with increasing T , achieved maximum values, and then decreased. Such behavior is in keeping with mixtures or block copolymers that would exhibit a closed-loop phase behavior.

Consequently, the differences in phase behavior between the blend and diblock copolymer of dPS and PnPMA originate in the differences in the temperature dependence of χ . However, the origin of this difference is not known. In addition, the absolute values of χ are not much different in the two cases. Subtle changes in the entropic contribution to χ could be an origin of this behavior.

The phase behavior of PS/PnPMA depends strongly on molecular weight. Changing M_w by only ~10% markedly alters phase diagram. According to the incompressible mean-field model, the critical value of $(\chi V/V_{\text{ref}})_{c,\text{block}}$ for the microphase separation of a symmetric block copolymer is 10.495.²³ Here, V is the total volume ($V_{\text{PS}} + V_{\text{PnPMA}}$) and V_{ref} is the reference volume (usually taken as the $(v_{\text{sp,PS}}[M]_{0,\text{PS}} v_{\text{sp,PnPMA}}[M]_{0,\text{PnPMA}})^{1/2}$) where

$v_{sp,i}$ and $[M]_{0,i}$ ($i = \text{PS, PnPMA}$) are the specific volume and monomer molecular weight of component i , respectively. $(\chi V_{\text{PS}}/V_{\text{ref}})_{\text{c,blend}} \approx (\chi V_{\text{PnPMA}}/V_{\text{ref}})_{\text{c,blend}} = 2$ for macrophase separation of a symmetric blend.¹ Because of the similarity in densities of PS and PnPMA, V/V_{ref} is directly proportional to M_w . The range in M_w of PS–PnPMA diblock copolymers where a closed loop is seen is quite narrow, ranging from 48 000 to 51 000.²⁰ $(\chi V)_{\text{c,copolymer}}/(\chi V_{\text{PS}})_{\text{c,blend}}$ ranges from 6.96 to 7.39, which is higher than theoretical value of 5.25 (10.495/2).

The failure of the mean-field arguments may arise if χ in the blend is different from that in the block copolymer, as discussed by Bates and co-workers.²⁵ Alternatively, Fredrickson and Helfand have argued that for finite molecular weights diblock copolymers $(\chi V/V_{\text{ref}})_{\text{c}} = 10.495 + 42.022\tilde{N}^{-1/3}$.²⁴ Here, \tilde{N} is the reduced number of chain segments $N[(b_{\text{PS}}^6/v_{\text{PS}}^2)(b_{\text{PnPMA}}^6/v_{\text{PnPMA}}^2)]^{1/2}$, where b_i and v_i are Kuhn length and monomer volume of component i . Consequently, $(\chi V/V_{\text{ref}})_{\text{c}} = 10.495 + 42.022 \cdot (862)^{-1/3} = 14.91$, which yields $(\chi V)_{\text{c,copolymer}}/(\chi V_{\text{PS}})_{\text{c,blend}} = 7.46$, which is slightly larger than the experimental value. It should be noted that, due to small value of \tilde{N} , this equation may not be valid because of the breakdown of Hartree approximation. Finally, both PS/PnPMA blend or PS–PnPMA block copolymer are compressible; thus, the exact value of $(\chi V/V_{\text{ref}})_{\text{c}}$ for blend (or block copolymer) might be different from 2.0 (or 10.5), respectively. The differences in the temperature dependence of χ for mixture and block copolymer have been discussed previously by Dudowicz and Freed^{12b} for PS–*block*–poly(vinyl methyl ether) [PS–PVME] and PS/PVME blend.

Although equations of state^{2,11,13} and lattice cluster theories with structured monomers¹² have been used to describe phase behavior with both UCST and LCST, parameters used in those theories are usually obtained after fitting experimental data. Thus, in this study, we compared the experimental results with predictions using by a compressible, regular solution theory, where all parameters are easily estimated or determined experimentally.^{15,16} According to this theory, the stability criterion for the mixed state is given by

$$\frac{\partial^2 g}{\partial \phi_A^2}|_{T,P,\tilde{\rho}} = kT \left[\frac{\tilde{\rho}_A}{\phi_A N_A v_A} + \frac{\tilde{\rho}_B}{\phi_B N_B v_B} \right] - 2[\tilde{\rho}_A \tilde{\rho}_B (\delta_{A,0} - \delta_{B,0})^2 + (\tilde{\rho}_A - \tilde{\rho}_B)(\delta_A^2 - \delta_B^2)] > 0 = A - 2B \quad (1)$$

where g is the free energy of mixing, ϕ_i is the volume fraction of component i with N_i segments of hard core volume v_i , k is the Boltzmann constant, and T is the temperature. The reduced density $\tilde{\rho}_i$ is given by $\rho_i N_{\text{AV}} v_i / M_{u,i}$, where $M_{u,i}$ is the molecular weight of monomer i with density ρ_i and N_{AV} is Avogadro's number. δ_i and $\delta_{i,0}$ are the cohesive energy and hard-core cohesive energy densities, respectively. The first term in eq 1 represents the configurational entropy, and the second term is the mean-field enthalpic contribution. The final term arises from difference in thermal expansion coefficients of the components (α_i). Once $\tilde{\rho}_i$ for two components are the same, eq 1 reduces to the spinodal criterion derived by the Flory–Huggins mean-field theory.

According to Mayes and co-workers,^{15,16} $\tilde{\rho}_i = \exp(-\alpha_i)$ and $\delta_{i,0} = \delta_i(298 \text{ K})/\tilde{\rho}_i(298 \text{ K})$. Also, $\delta_i(298 \text{ K})$ can be estimated by a group contribution.²⁶ From eq 1, the first term (A) decreases gradually with increasing

temperature, whereas term B exhibits two extremes, even though $B \geq 0$. With increasing temperature, the value of B first decreases, then increases, and finally decreases again. Thus, eq 1 has one minimum at a lower temperature (T_{min}) and one maximum at a higher temperature (T_{max}). This theory predicts that the blend system has UCST at a temperature lower than T_{min} , a closed loop type phase diagram with LCST at a temperature between T_{min} and T_{max} , and also an upper UCST at a temperature higher than T_{max} . Of course, the maximum stability (or maximum miscibility) occurs at T_{min} . As seen in eq 1, T_{min} and T_{max} depend on two parameters (α_i and $\delta_i(298 \text{ K})$). If $T_{\text{min}} < 0$, one can expect an LCST, even though an upper UCST might exist at very high temperatures.

α_{PS} and α_{PnPMA} , determined by measuring the thickness change of films as a function of temperature, were found to be 5.5×10^{-4} (1/K) and 7.7×10^{-4} (1/K), respectively.²¹ Notice that the value of α_{PS} is close to literature value²⁷ and that α for poly(*n*-alkyl methacrylate) is known to be larger than α_{PS} .²⁷ From a group contribution,²⁶ $\delta_{\text{PS}}(298 \text{ K}) \sim 18.198$ (J/cm³)^{1/2} and $\delta_{\text{PnPMA}}(298 \text{ K}) \sim 18.193$ (J/cm³)^{1/2}. Using these values, $T_{\text{min}} = 229 \text{ K}$ and $T_{\text{max}} = 1698 \text{ K}$. The predicted UCST, LCST, and upper UCST are 55 K, 457 K, and 5130 K, respectively, for the 50/50 wt/wt PS–L/PnPMA–L blend. Interestingly, the predicted LCST (457 K) is similar to experimental data (463 K) given in Figure 1, but the predicted value of the UCST (55 K) is too low compared with experimental value (360 K). It should be noted that the predicted T_{min} (229 K) is lower than the midpoint (256 K) of UCST and LCST, which is consistent with SANS results for the d-PS/PnPMA–M blend. However, while theory provides some insight into the phase behavior of the blend, agreement with experiments is not quantitative. For example, the theory predicts a UCST at 55 K and LCST at 451 K for the 50/50 wt/wt PS–H/PnPMA–L blend system. But experiments show that the blend is macrophase-separated over the entire temperature range (namely within an hourglass window).

In the summary, it has been shown that weakly interacting PS/PnPMA blends exhibit both UCST and LCST behavior. With only a slight increase in M_w of PS, a transition to an hourglass type of phase behavior was found. This interesting phase diagram of the PS/PnPMA blend was due to a nonlinear dependence of χ on inverse temperature. Namely, with increasing temperature, χ of PS/PnPMA measured by SANS first decreases, goes through a minimum, and then increases again.

Acknowledgment. This work was supported by the Hanaro program, the National Research Laboratory Program, the Applied Rheology Center governed by KOSEF, the National Science Foundation sponsored by Materials Research Science and Engineering Center at the University of Massachusetts (DMR9809365), the Department of Energy, Office of Basic Energy Sciences. Small-angle neutron scattering was performed at the Hanaro SANS beam line supported by KAERI.

References and Notes

- Paul, D. R.; Newman, S., Eds.; *Polymer Blends*; Academic Press: New York, 1978.
- Sanchez, I. C. In *Polymer Compatibility and Incompatibility*; Solc, K., Ed.; MMI Press: New York, 1982.
- Koningsveld, R.; Stockmayer, W. H.; Nies, E. *Polymer Phase Diagram*; Oxford University Press: New York, 2001.
- Saeki, S.; Kuwahara, N.; Konno, S.; Kaneko, M. *Macromolecules* **1973**, *6*, 246.

- (5) Ougizawa, T.; Inoue, T.; Kammer, H. W. *Macromolecules* **1985**, *18*, 2089.
- (6) Cong, G.; Huang, Y.; MacKnight, W. J.; Karasz, F. E. *Macromolecules* **1986**, *19*, 2765.
- (7) Hammouda, B.; Bauer, B. J.; Russell, T. P. *Macromolecules* **1994**, *27*, 2357.
- (8) Russell, T. P.; Karis, T. E.; Gallot, Y.; Mayes, A. M. *Nature (London)* **1994**, *368*, 729.
- (9) McMaster, L. P. *Macromolecules* **1973**, *6*, 760.
- (10) Patterson, D.; Robard, A. *Macromolecules* **1978**, *11*, 690.
- (11) Sanchez, I. C.; Lacombe, R. H. *Macromolecules* **1978**, *11*, 1145.
- (12) (a) Dudowicz, J.; Freed, K. F. *Macromolecules* **1991**, *24*, 5076. (b) Dudowicz, J.; Freed, K. F. *Macromolecules* **1993**, *26*, 213.
- (13) Hino, T.; Prausnitz, J. M. *Macromolecules* **1998**, *31*, 2636.
- (14) Cho, J. *Macromolecules* **2000**, *33*, 2228.
- (15) Ruzette, A. V. G.; Mayes, A. *Macromolecules* **2001**, *34*, 1894.
- (16) Ruzette, A. V. G.; Banerjee, P.; Mayes, A. M.; Pollard, M.; Russell, T. P. *J. Chem. Phys.* **2001**, *114*, 8205.
- (17) Bates, F. S.; Wignall, G. D.; Koehler, D. K. *Phys. Rev. Lett.* **1985**, *55*, 2425.
- (18) Balsara, N. P. In *Physical Properties of Polymers Handbook*; Mark, J. E., Ed.; AIP Press: Secaucus, NJ, 1997; Chapter 19.
- (19) Graessley, W. W.; Krishnamoorti, R.; Reichart, G.; Balsara, N. P.; Fetters, L. J.; Lohse, D. J. *Macromolecules* **1995**, *28*, 1260.
- (20) Ryu, D. Y.; Jeong, U.; Kim, J. K.; Russell, T. P. *Nature Mater.* advanced online publication, 02/09/2002 (DOI: 10.1038/nmat724).
- (21) Ryu, D. Y.; Kim, J. K. Unpublished results, 2001.
- (22) de Gennes, P. G. *Scaling Concepts in Polymer Physics*; Cornell University Press: Ithaca, NY, 1979.
- (23) Leibler, L. *Macromolecules* **1981**, *13*, 1602.
- (24) Fredrickson, G. H.; Helfand, E. *J. Chem. Phys.* **1987**, *87*, 697.
- (25) Maurer, W. W.; Bates, F. S.; Lodge, T. P.; Almdal, K.; Mortensen, K.; Fredrickson, G. H. *J. Chem. Phys.* **1998**, *108*, 2989.
- (26) Van Krevelen, D. W.; Hoftyzer, P. J. *Properties of Polymer*, 2nd ed.; Elsevier: New York, 1976.
- (27) Zoller, P.; Walsh, D. J. *Standard Pressure–Volume–Temperature Data for Polymers*; Technomic Pub.: Lancaster, 1995.

MA025615Q